


FULL PAPER

Open Access



Spatial and temporal influence of sea level on inland stress based on seismic velocity monitoring

Rezkiya Dewi Andajani^{1,2*} , Takeshi Tsuji^{1,2,3}, Roel Snieder⁴ and Tatsunori Ikeda^{2,3}

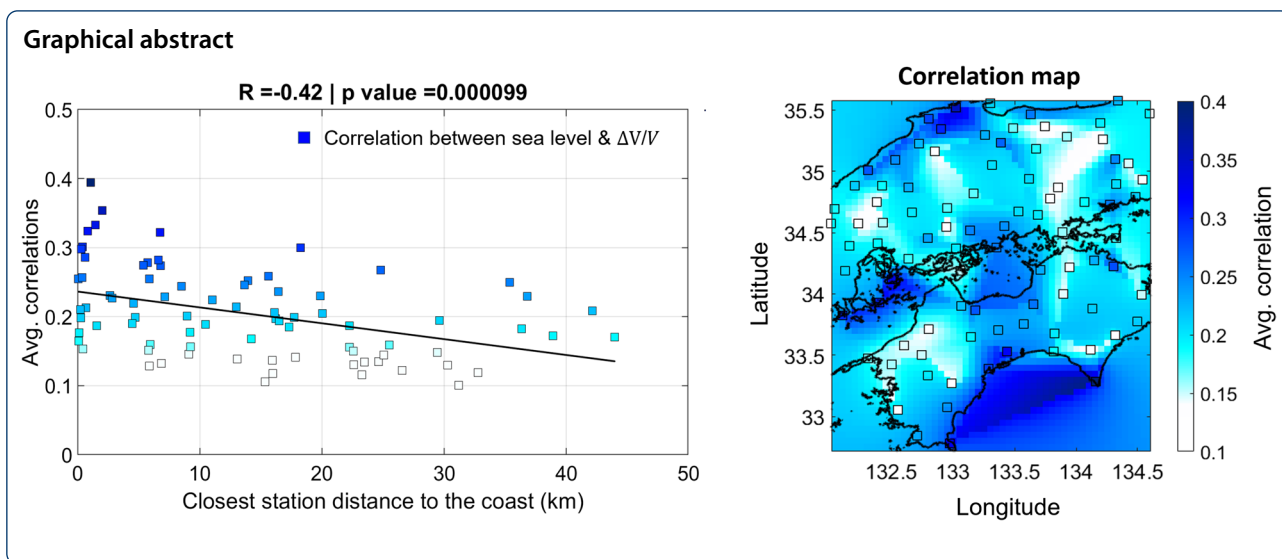
Abstract

Earth's crust responds to perturbations from various environmental factors. To evaluate this response, seismic velocity changes offer an indirect diagnostic, especially where velocity can be monitored on an ongoing basis from ambient seismic noise. Investigating the connection between the seismic velocity changes and external perturbations could be useful for characterizing dynamic activities in the crust. The seismic velocity is known to be sensitive to variations in meteorological signals such as temperature, snow, and precipitation as well as changes in sea level. Among these perturbations, the impact of variations in sea level on velocity changes inferred from seismic interferometry of ambient noise is not well known. This study investigates the influence of the ocean in a 3-year record of ambient noise seismic velocity monitoring in the Chugoku and Shikoku regions of southwest Japan. First, we applied a bandpass filter to determine the optimal period band for discriminating among different influences on seismic velocity. Then, we applied a regression analysis between the proximity of seismic station pairs to the coast and the ocean influence, as indicated by the correlation of sea level to seismic velocity changes between pairs of stations. Our study suggests that for periods between 0.0036 to 0.0155 cycle/day (64–274 days), the ocean's influence on seismic velocity decreases with increasing distance of station pairs from the coast. The increasing sea level deforms the ocean floor, affecting the stress in the adjacent coast. The stress change induced by the ocean loading may extend at least dozens of kilometers from the coast. The correlation between sea level and inland seismic velocity changes is negative or positive. Although it is difficult to clearly interpret the correlation based on a simple model, they could depend on the in situ local stress, orientation of dominant crack, and hydraulic conductivity. Our study shows that seismic monitoring may be useful for evaluating the perturbation in the crust associated with an external load.

Keywords: Seismic velocity change, Sea level change, Ocean loading, Inland deformation

*Correspondence: rezkia@sys.t.u-tokyo.ac.jp

¹ Department of Systems Innovation, The University of Tokyo, 731 Hongo Bunkyo-ku, Tokyo 113-8656, Japan
Full list of author information is available at the end of the article



Introduction

The understanding of how the Earth’s crust responds to various environmental perturbations is important for earthquake evaluations, geological storage facilities, and geothermal developments. Temporal variations in seismic velocity can be linked to the activities of volcanoes and earthquakes (e.g., Hutapea et al. 2020; Nimiya et al. 2017; Rivet et al. 2014; Takano et al. 2017). They are also sensitive to surface perturbations associated with climatic perturbations such as rainfall (Nakata and Snieder 2012; Sens-Schönfelder and Wegler 2006; Andajani et al. 2020), snow (Mordret et al. 2016), atmospheric pressure (Niu et al. 2008; Silver et al. 2007), and temperature (Hillers et al. 2015; Richter et al. 2014). The influence of environmental perturbations on seismic velocity changes can be presumed to differ for various locations. For example, since volcanic regions are sensitive to internal and external forcing (e.g., Albino et al. 2010; Matthews et al. 2009; Neuberg 2000), seismic velocity changes in volcanic regions should be analyzed in terms of surface perturbations as well as magmatic and tectonic activities (e.g., Donaldson et al. 2019). Precipitation dominates the temporal seismic velocity changes in locations where groundwater is rapidly recharged (e.g., Andajani et al. 2020; Sens-Schönfelder and Wegler 2006). In arid regions, temperature is likely to dominate the variations of seismic velocity (Hillers et al. 2015). The influence of atmospheric pressure is likely to apply to any location, and its effect is observable as deep as seismogenic depths (Niu et al. 2008).

A previous study has shown that precipitation, snow, and sea level influence the crustal deformation of the Japan Islands as detected by ambient noise correlation (Wang et al. 2017). It is less well known how changes in

sea level, such as its current global sea level rise, affect seismic velocity changes. The crust of Japan is known to be affected by the loading from the ocean (Hatanaka et al. 2001; Sato et al. 2001); thus, we seek in this study to better characterize the effect of sea level variations on estimated seismic velocity changes by considering its spatial variation.

This work is a continuation of our research on the interpretation of seismic velocity changes from ambient noise in the Chugoku and Shikoku regions of southwest Japan (Andajani et al. 2020). The study region is surrounded by the Seto inland sea, Japan Sea, and the Pacific coast. This region lacks active volcanoes and is subject to heavy rain, where water can be directly discharged to the coast by rivers if there is no rainfall infiltration. Snow is uncommon and its influence can thus assumed to be negligible.

The influence of the ocean should be strongest in the coastal environment and should decrease with increasing distance to the ocean. In this study, we seek to estimate the spatial scale of this effect by searching for the period band where the relationship between sea level variability and seismic velocity changes can best be identified. We find that in the period band from 64 to 274 days (0.0036 – 0.0155 cycle/day), the influence of sea level on seismic velocity change tends to decrease with the increasing station’s distance from the coast. We interpret this result as inland stress changes induced by ocean loading.

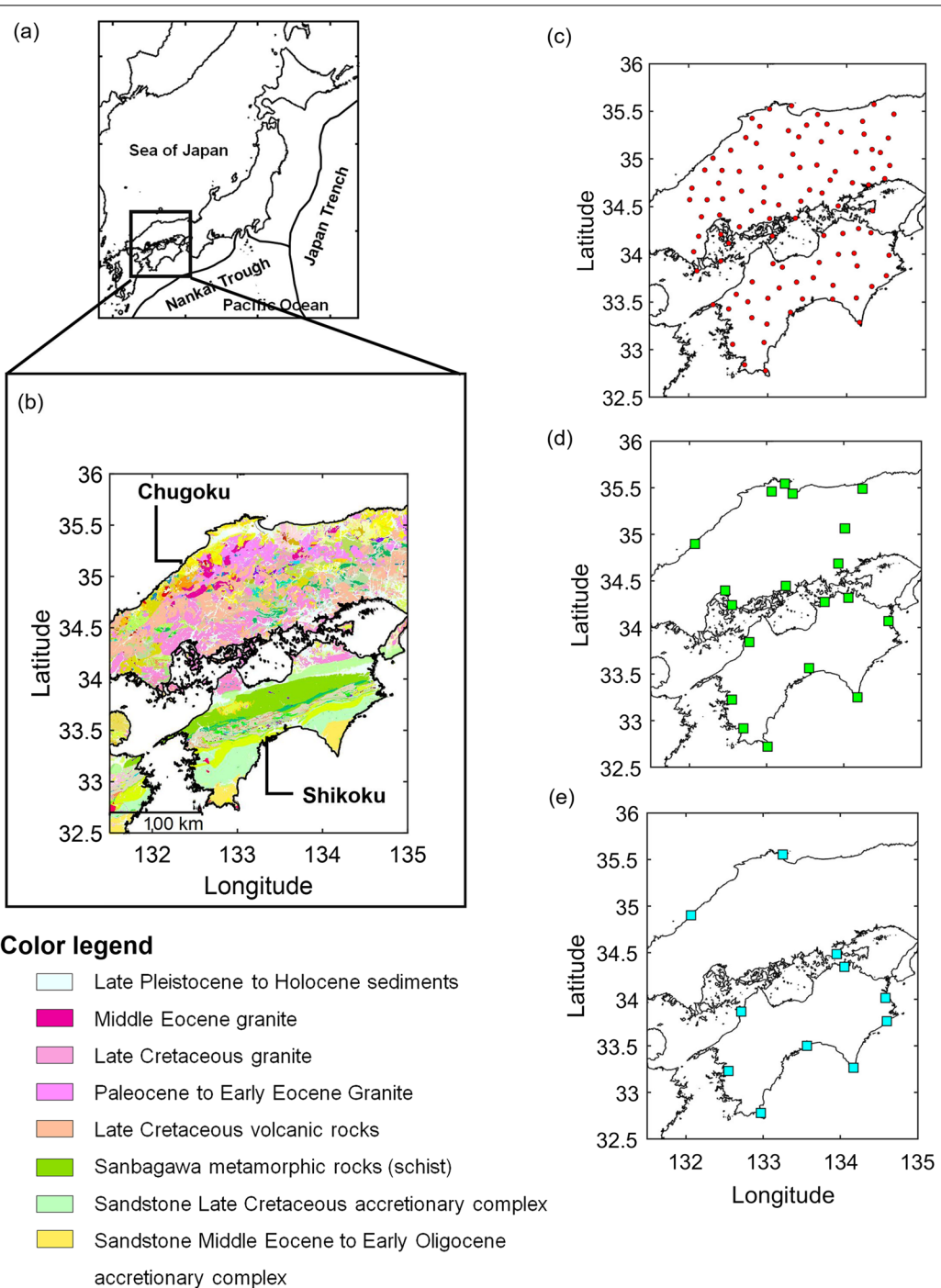


Fig. 1 **a** Location map of Japan showing the study area in the Chugoku and Shikoku regions, **b** bedrock map of the study region (modified from the Geological Survey of Japan AIST 2015), and location maps of **c** seismic stations, **d** atmospheric pressure gauges, and **e** ocean tidal observations

Data preparation

We used seismic data for 99 Hi-net seismic stations in Chugoku and Shikoku (Fig. 1) from the National Research Institute for Earth Science and Disaster Resilience (NIED) (Obara et al. 2005). The Chugoku region is composed chiefly of volcanic and granitic rocks, whereas Shikoku Island consists mostly of the Sanbagawa metamorphic belt and multiple accretionary complexes (Fig. 1b). Using seismic velocity changes estimated from ambient noise for 306 station pairs, we compared the time series of seismic velocity change to meteorological data for the same region during the years 2015–2017. We used sea level and atmospheric pressure data recorded by the Japan Meteorological Agency (JMA) along the Chugoku and Shikoku coasts (Fig. 1d and e).

Our study utilized seismic velocity changes inferred from the coda of the cross-correlation of the recorded vertical component of ambient noise. We analyzed ambient noise data in the seismic frequency range from 0.1–0.9 Hz. The daily ambient noise data were divided into 30-min segments with 50% overlap. Assuming Rayleigh waves are dominant in the coda of the cross-correlation, the seismic velocity change reflects the variations of S-wave velocity within 1–8 km depth (e.g., Andajani et al. 2020; Nimiya et al. 2017). The time window of 100 s of the coda wave was selected. The starting time of the window was determined as $t_{start} = d/v_{min}$ where d is the distance between station pairs (maximum is 40 km) and v_{min} is the minimum apparent velocity between pair of stations ($v_{min} = 1$ km/s). Around frequency range of 0.1–0.9 Hz, surface wave propagates ~ 2 km/s in Chugoku region (e.g., Suemoto et al. 2020). By choosing the slower velocity around 1 km/s than the direct surface waves, we selected the coda parts (e.g., Meier et al., 2010). Seismic velocity changes were estimated with stretching interpolation method (Hadziioannou et al. 2009; Hutapea et al. 2020; Minato et al. 2012; Nimiya et al. 2017) where one maximizes:

$$CC(\varepsilon) = \frac{\int f_{\varepsilon}^{cur}(t) f^{ref}(t) dt}{\left(\int (f_{\varepsilon}^{cur}(t))^2 dt \int (f^{ref}(t))^2 dt \right)^{1/2}}, \quad (1)$$

with

$$f_{\varepsilon}^{cur}(t) = f^{cur}(t(1 + \varepsilon)), \quad (2)$$

where f^{ref} represents the reference trace, f^{cur} is the current trace, and t is time. The stretching interpolation method elongates the time axis and searches for traces similar to the reference trace based on the correlation coefficient $CC(\varepsilon)$. To stabilize the monitoring result over the 3-year term, we analyzed the seismic velocity change in each year individually by using the sliding reference

method (SRM) (Hutapea et al. 2020). We defined the reference trace f^{ref} as the 1-year stack of coda of cross-correlation data and used the 10-day stack of coda of cross-correlation as the current trace f^{cur} . The stretching parameter ε is related to the relative time shift ($\Delta t/t$) and the velocity change ($\Delta v/v$) described in

$$\varepsilon = \Delta t/t = -(\Delta v/v). \quad (3)$$

The average stretching correlation coefficients for all estimated seismic station pairs are shown in Figure S1 of the additional file 1. The lowest stretching correlation coefficient is ~ 0.5 . Most of the station pairs (210 of 306) have stretching correlation coefficients greater than 0.6, indicating that the estimated seismic velocity changes in the Chugoku and Shikoku regions are well-constrained (e.g., Ikeda and Takagi, 2019; Yukutake et al. 2016).

The observed sea level is a composite of geophysical cycles that include tidal variations (astronomical tides), non-tidal variations (meteorological contributions), and mean sea levels (Haigh 2017). We computed our time series of daily sea level by averaging 24 h of data (Additional file 1: Figure S2a). Averaging the hourly sea level over each day tends to suppress semidiurnal and diurnal variations, although longer period variations such as the fortnightly lunar or semiannual solar cycle may remain. Because the amplitudes of these long-period cycles of the astronomical tide are small, sea level variation is usually dominated by the non-tidal processes (Woodworth et al. 2019). Thus, we took the dominance of non-tidal processes in sea level variability as an assumption. As for the atmospheric pressure, we directly collected the data from JMA.

Methods

Our investigation of the influence of sea level changes on seismic velocity changes comprised three steps (Fig. 2). The first step was to distinguish the respective cycles of sea level and atmospheric pressure. Sea level and atmospheric pressure tend to have dominant cycles that are similar, as indicated by Pearson correlation coefficients as great as -0.68 (Additional file 1: Figure S2). The correlation between these two time series raises a difficulty in unraveling the contribution of sea level and atmospheric pressure on seismic velocity. Therefore, we searched for the optimum period bands in the dataset to distinguish the two cycles. Once the best period band was identified, in step 2 we estimated the influence of sea level on seismic velocity by calculating the Pearson correlation coefficient of the two time series after filtering by that period band. Correlation coefficients were calculated for each seismic station pair. Finally, in step 3, we evaluated the relationship between correlation coefficients and the

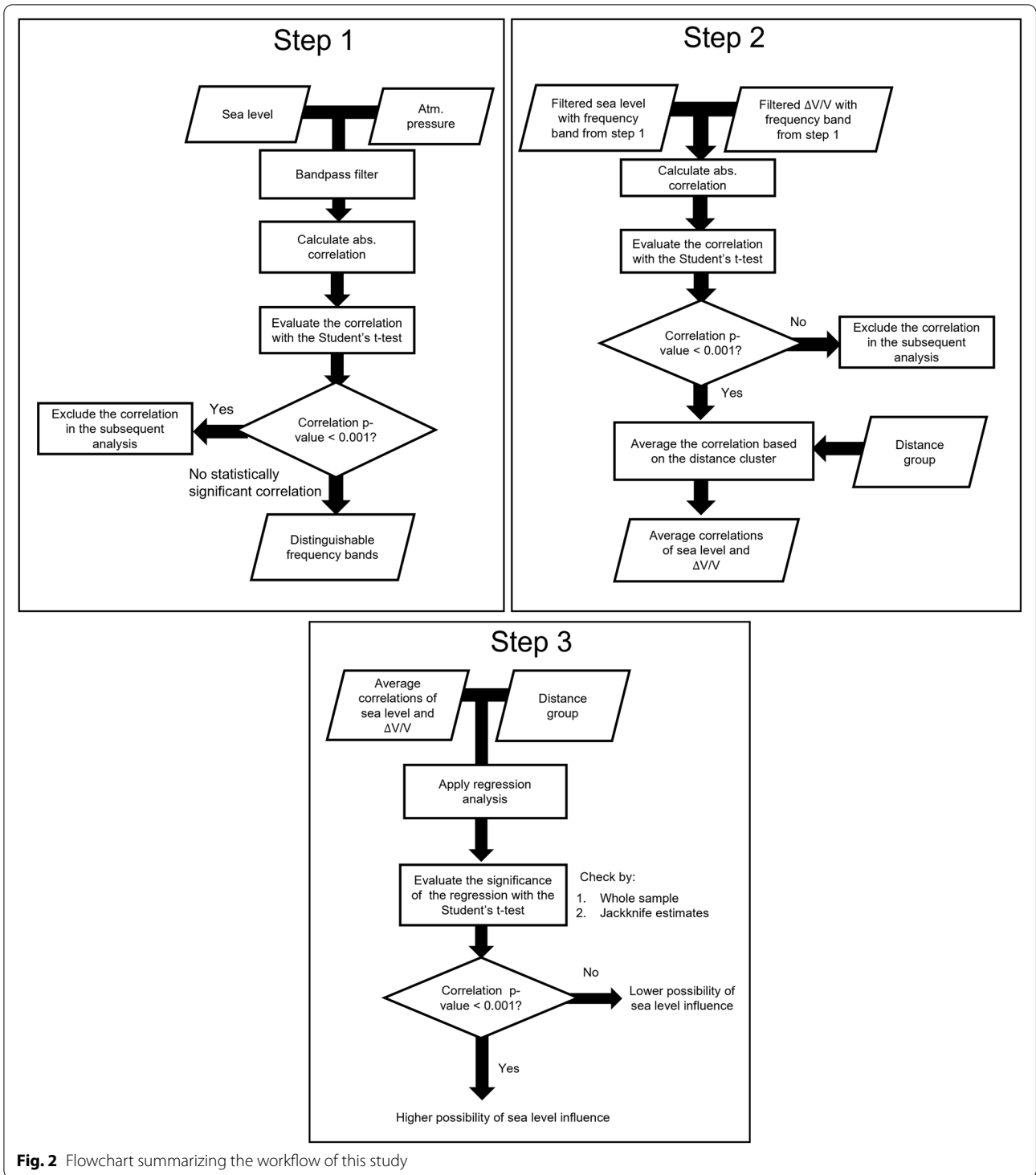
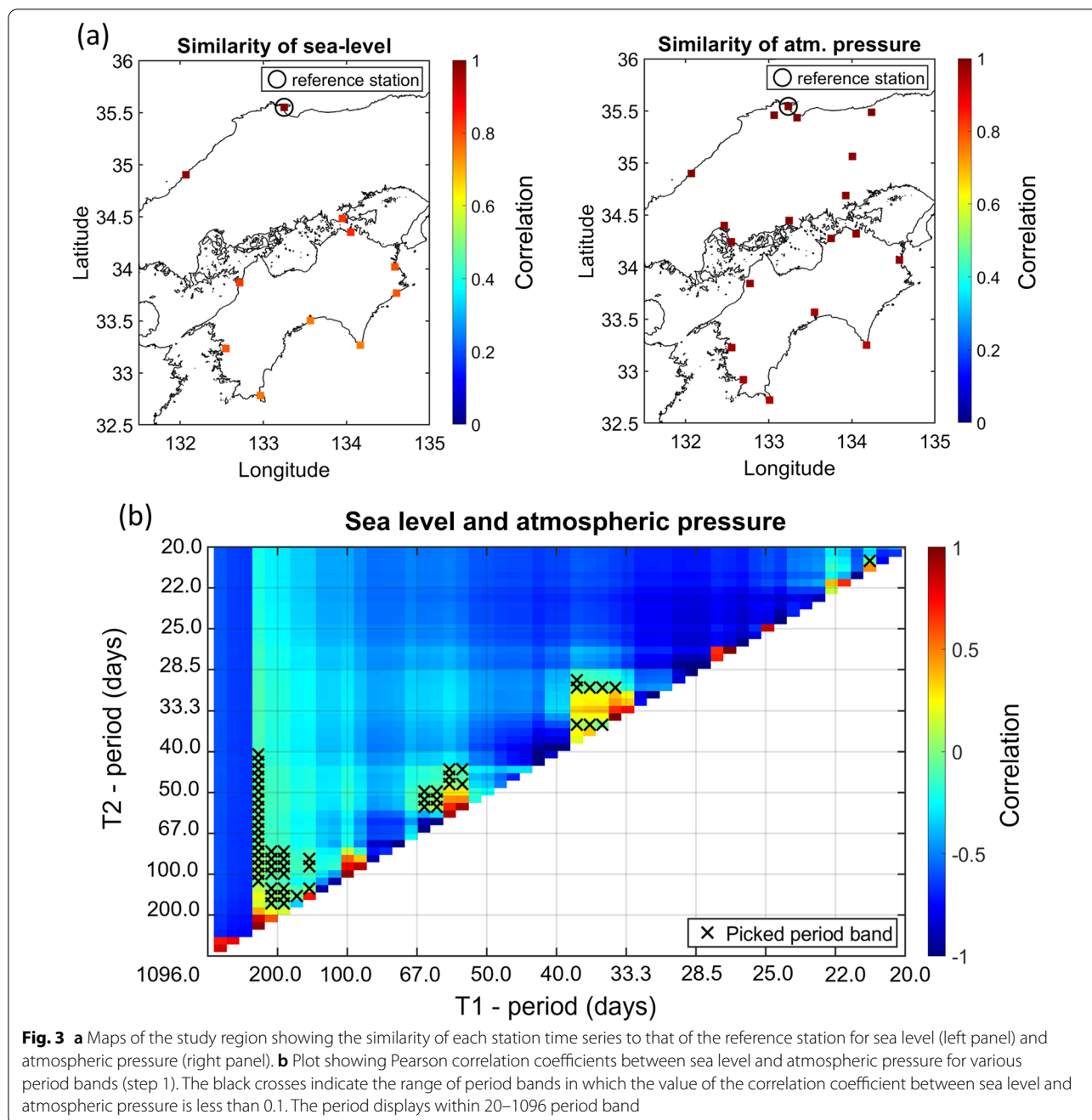


Fig. 2 Flowchart summarizing the workflow of this study

distance of seismic stations to the coast. Considering that the ocean caused perturbations on the seabed and the nearby shore, we searched for the possibility of decreasing correlations obtained from step 2 with increasing

distance from the ocean. Assuming a linear relationship, we used a statistical approach to evaluate the evidence of decreasing correlations with increasing distance from the coast.



Step 1: distinguishing cycles of sea level and atmospheric pressure

Atmospheric pressure loading can cause crustal displacement. Because atmospheric pressure exerts a load on both inland and coastal regions (e.g., Gladkikh et al. 2011; van Dam et al. 1994), it is necessary to distinguish the imprint of the sea level variations on seismic velocity changes from the influence of atmospheric pressure fluctuations. For both sea level and atmospheric

pressure, we calculated the correlation coefficient between the data from the reference station (black circle in Fig. 3a) and those from other stations (square in Fig. 3a). Because high values of correlation coefficients indicate the time series from other stations are similar to the reference station (Fig. 3a), and the time series from all stations are similar (Additional file 1: Figure S2a,b), we averaged the sea level and atmospheric pressure from all stations independently (Additional

file 1: Figure S2c,d). We then applied a bandpass filter and calculated the Pearson correlation coefficients between the two resulting time series. We searched for the period bands where the sea level cycle was most weakly correlated with atmospheric pressure. We limited the search to periods between 3 years and 10 days (~0.000912–0.1 cycle/day). The 10-day limit was chosen on the basis of the 10-day stacking data of current traces (f^{cur}) used to estimate seismic velocity changes.

We further evaluated the significance of the correlation between sea level and atmospheric pressure with Student’s t -test, which has been used in geophysical studies (e.g., Hunt et al. 2014; Kalkomey 1997; Khandelwal 2013). The value of t is defined by

$$t\text{-value} = \frac{(R\sqrt{n-2})}{(\sqrt{1-R^2})}, \tag{4}$$

where n is the number of samples, and R is the Pearson correlation coefficient. We used two hypotheses in this evaluation, the null hypothesis ($H_0, R = 0$) and the alternative hypothesis ($H_1, R \neq 0$). Two types of error might occur while testing the null hypothesis: type I error, in which we incorrectly reject the null hypothesis (false positive), and type II error, in which the null hypothesis is false but we fail to reject it (false negative). The probability of making a type I error is defined as significance level α .

When testing H_1 , we compared the probability value (p -value) with the significance level α to evaluate whether the correlation of two time series was due to chance or not. The p -value of our estimated t -value in Eq. 4 was obtained from the Student’s t -distribution table. Since we tested the evidence for $R \neq 0$, we used a double-tailed Student’s t -distribution. If our p -value is smaller than the significance level α , the null hypothesis can be rejected. The choice of α is arbitrary. The greater the sample size, the more likely a significant relationship will be correctly identified if one exists (Thiese et al. 2016); however, a large sample size may also cause a nonsignificant relationship to appear statistically significant (p -value $< \alpha$). Hence, a low significance level, such as 0.005 or 0.001, is preferred for a large sample size (Kim and Choi 2019). In this case, we considered the sample size as 1096 days observation.

The correlation coefficients between sea level and atmospheric pressure are close to zero in several period ranges (Fig. 3b). For 3-year observation, the p -value for the correlation smaller than 0.1 is larger than $\alpha=0.001$. Any correlation smaller than 0.1 is considered statistically insignificant. Since we aimed to separate the cycles of sea level and atmospheric pressure, we sought a period band in which the correlation coefficient was less

than a threshold value of 0.1 (black crosses in Fig. 3b). This period band occupied the range of 12.5–274 days (~0.0036–0.08 cycle/day). We used this period band for filtering the time series of seismic velocity changes and sea level changes in step 2.

Step 2: evaluating the sea level influence on seismic velocity changes

We applied a bandpass filter using the period band from step 1 to the time series of sea level and seismic velocity changes for each seismic station pair. We then calculated the absolute Pearson correlation coefficients between the filtered sea level and seismic velocity changes. Following step 1, we evaluated the significance of the correlation coefficient between seismic velocity changes and sea level changes through Student’s t -test. In this step, we included only statistically significant correlation coefficient (p -value < 0.001) between sea level and seismic velocity changes in the subsequent analysis.

We assumed the observed seismic velocity change between a pair of stations as the average velocity change at two stations (Hobiger et al. 2012; Ikeda and Tsuji 2018) because the kernel’s sensitivity peak would be equally high at both stations (e.g., Pacheco and Snieder 2005, 2006). We expect the seismometer located closer to the coast would be more strongly influenced by ocean perturbations. Therefore, for each seismic station pair, we defined the distance between the coast and the seismometer that was located closest to the coast (Fig. 4a), and then used those distances to group the station pairs with the same distance, resulting in 92 distance clusters (Fig. 4b). Once we grouped the station pairs, we

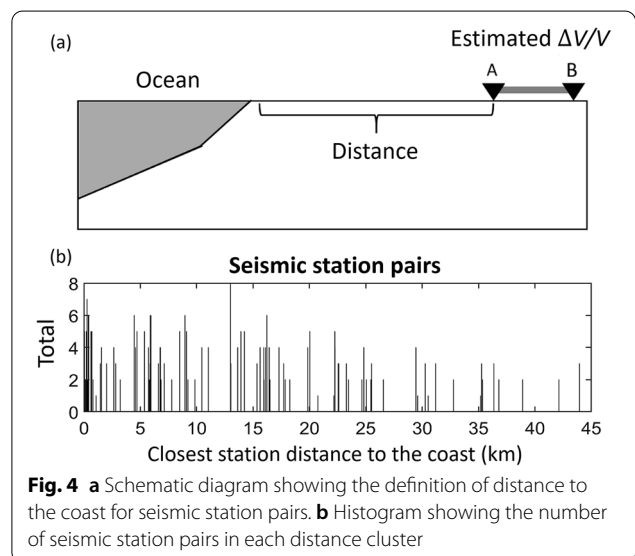


Fig. 4 a Schematic diagram showing the definition of distance to the coast for seismic station pairs. b Histogram showing the number of seismic station pairs in each distance cluster

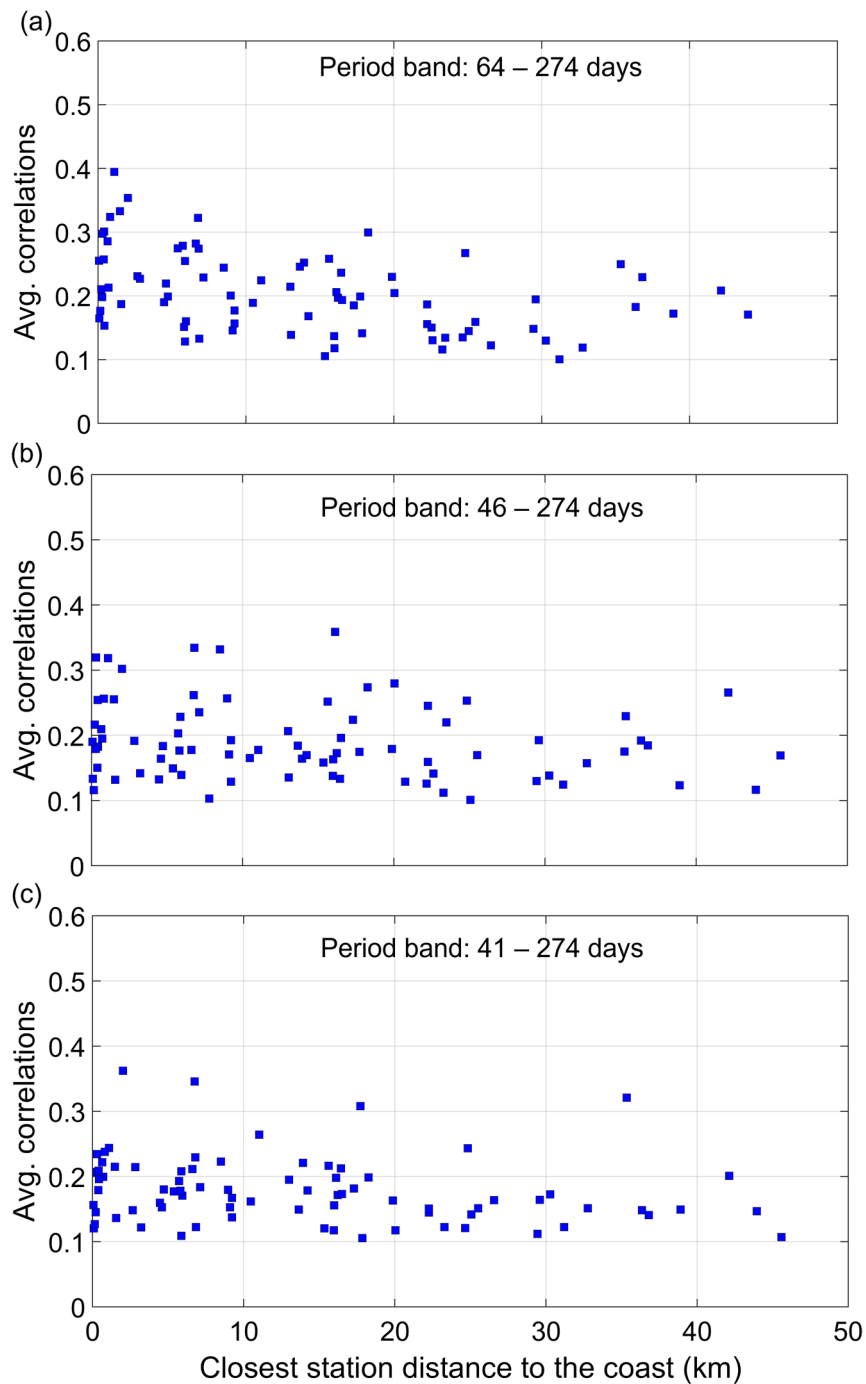


Fig. 5 Scatterplots between the average absolute correlation between sea level and seismic velocity change and the distance from the coast for period bands of **a** 64–274, **b** 46–274, and **c** 41–274 days

averaged the absolute correlation coefficients within each distance cluster (Fig. 5). The resulting scatterplot indicated a trend of decreasing correlations with increasing coastal distance in the time series filtered within the

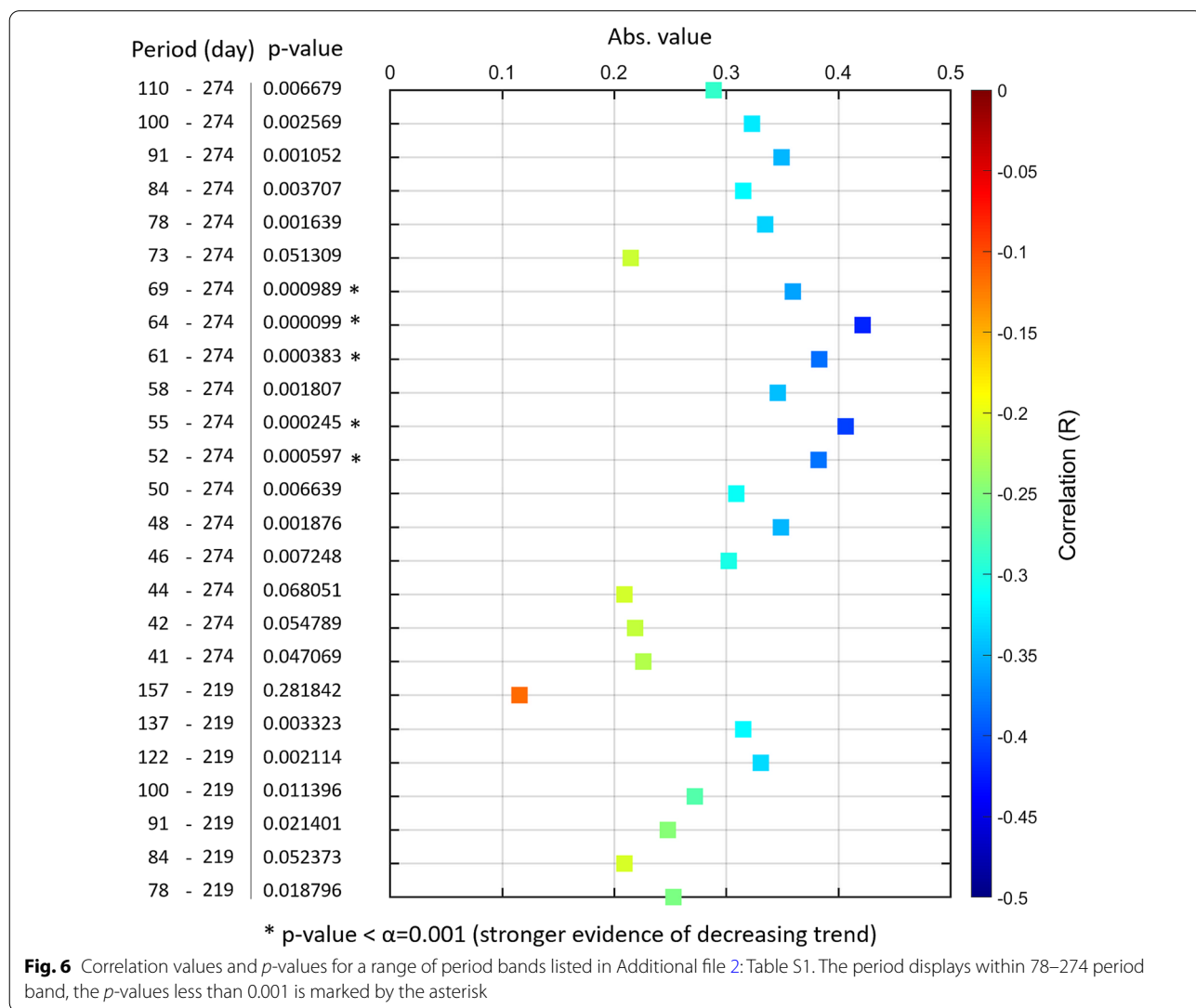
range of 64–274 days (Fig. 5a). At wider filtering period bands (e.g., 46–274 to 41–274 days), the decreasing trend was weaker (Fig. 5b and 5c). This finding suggests that

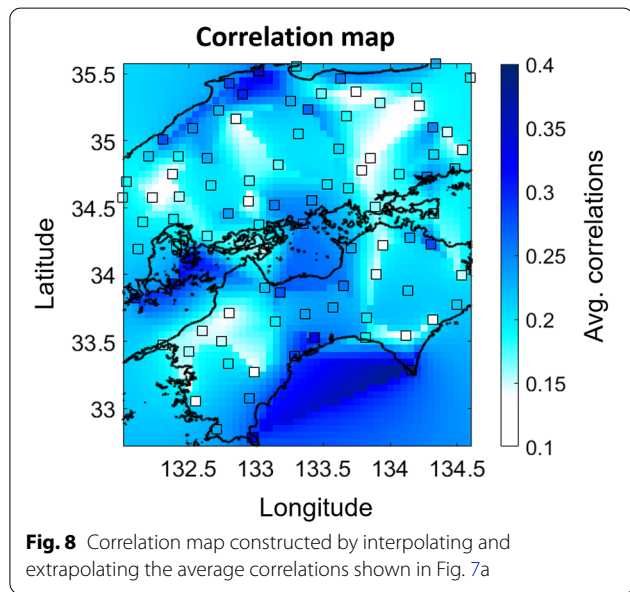
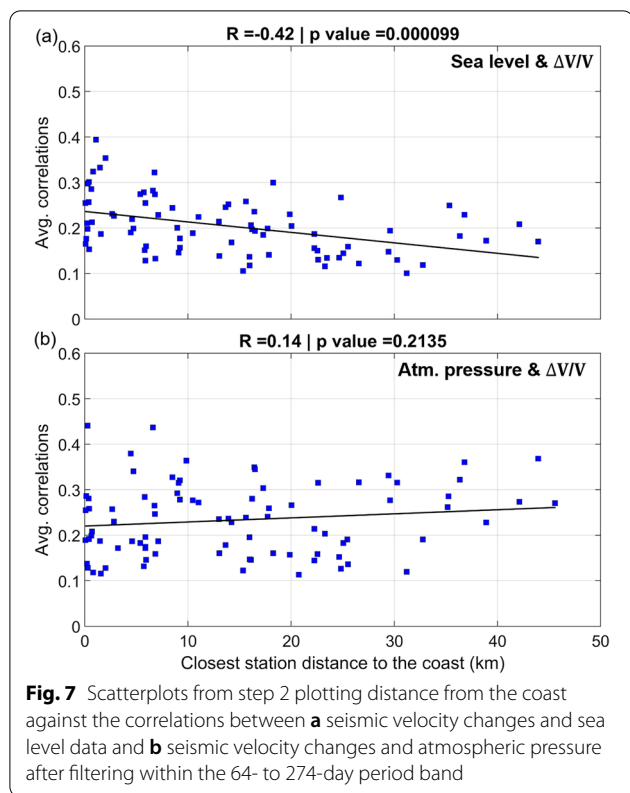
the influence of sea level is observable only in a limited period band.

Step 3: evaluating the significance of the decreasing trend

Under the assumption that the influence of ocean loading decreases away from the coast, we evaluated the optimum period band where the influence of sea level was strongest by testing the hypothesis of a linear relationship between the correlation coefficient and distance to the coast. We defined the dependent variable Y_i as the averaged absolute correlations and the independent variable X_i as the distance to the coast (of 92 distance bins). We then calculated the t -value for the scatterplots in step 2 between X_i . With the total sample consisting of 92 distance clusters, we adopted a significance level α of 0.001.

After the best frequency band was determined by the t -test, we further compared the correlation coefficient between X_i and Y_i from the whole sample with the correlation estimated through jackknife estimates. In the jackknife estimates, one element from the original sample is omitted prior calculating the correlation coefficient. As we have 92 elements ($n=92$) of the variables X_i and Y_i , we omitted the first element and estimated the correlation coefficient between X_i and Y_i for $n-1$ (R_1). Then, the second element was omitted from the original 92 elements and the correlation coefficient (R_2) was re-calculated. This procedure was repeated until we obtained 92 correlation coefficients (R_1, \dots, R_{92}).





Results

Figure 6 shows examples of scatterplots evaluated from the whole sample based on the period bands from step

1. Additional file 2: Table S1 shows the results for all possible period bands. The R values are mostly negative. The trend of the scatterplot becomes statistically significant (p -value < 0.001) and the absolute correlations are larger as we increase the bandwidth to be within 52–274 days. When the shortest period is smaller than 52 days (e.g., 50–274 and 41–274 days), the correlation turns weaker with the p -value exceeds 0.001 (Fig. 6 and Additional file 2: Table S1).

The period bands with high absolute R and p -value $< \alpha$ indicate stronger evidence of a decreasing trend. The R estimated from the whole sample is the highest within 64 – 274 days period ($R = -0.42$) and statistically significant with p -value = 0.000099. For this period band, the correlation for all 92 jackknife replications varies within -0.4 to -0.45, with all the p -value smaller than 0.001. This confirms that the correlation is robust. Based on these results, we selected 64–274 days as the optimum period band (Fig. 7a). To emphasize the regional features of the correlations, we constructed a correlation map (Fig. 8) by interpolated and extrapolated the value of the correlations in Fig. 7a.

The correlation values between sea level and seismic velocity changes are shown in Fig. 9 for all seismic station pairs; 126 station pairs had statistically negative correlations (p -value < 0.001) and 62 pairs had statistically significant positive correlations between seismic velocity change and sea level (Fig. 9b and 9c, respectively). Additional file 1: Figures S3 and S4 shows examples of filtered and unfiltered time series used for station pairs with negative correlations 0.4 – 0.5 and positive correlations within 0.3–0.45, respectively.

Discussion

Assessment of correlation

For individual station pairs, a high correlation that we estimated is ~ 0.4 (e.g., Fig. 9, Additional file 1: Figures S3 and S4). In some cases, correlations above 0.4 ($R \geq 0.4$) are interpreted as relatively moderate strength (e.g., Akoğlu 2018; McBeck et al. 2020; Schober et al. 2018). This implies there is considerable influence of sea level on seismic velocity changes for some station pairs. However, the average correlation between sea level and seismic velocity changes filtered in 64 – 274 days were mostly 0.3. Although such value appears to be small, this correlation is significant. As checked by the Student’s t -test, a correlation > 0.1 is statistically significant at level of significance of 0.001. This indicates the correlation above 0.1 in our result was not due to chance, regardless of the weak correlation (≥ 0.1). The possibility of sea level changes influencing seismic velocity changes is further

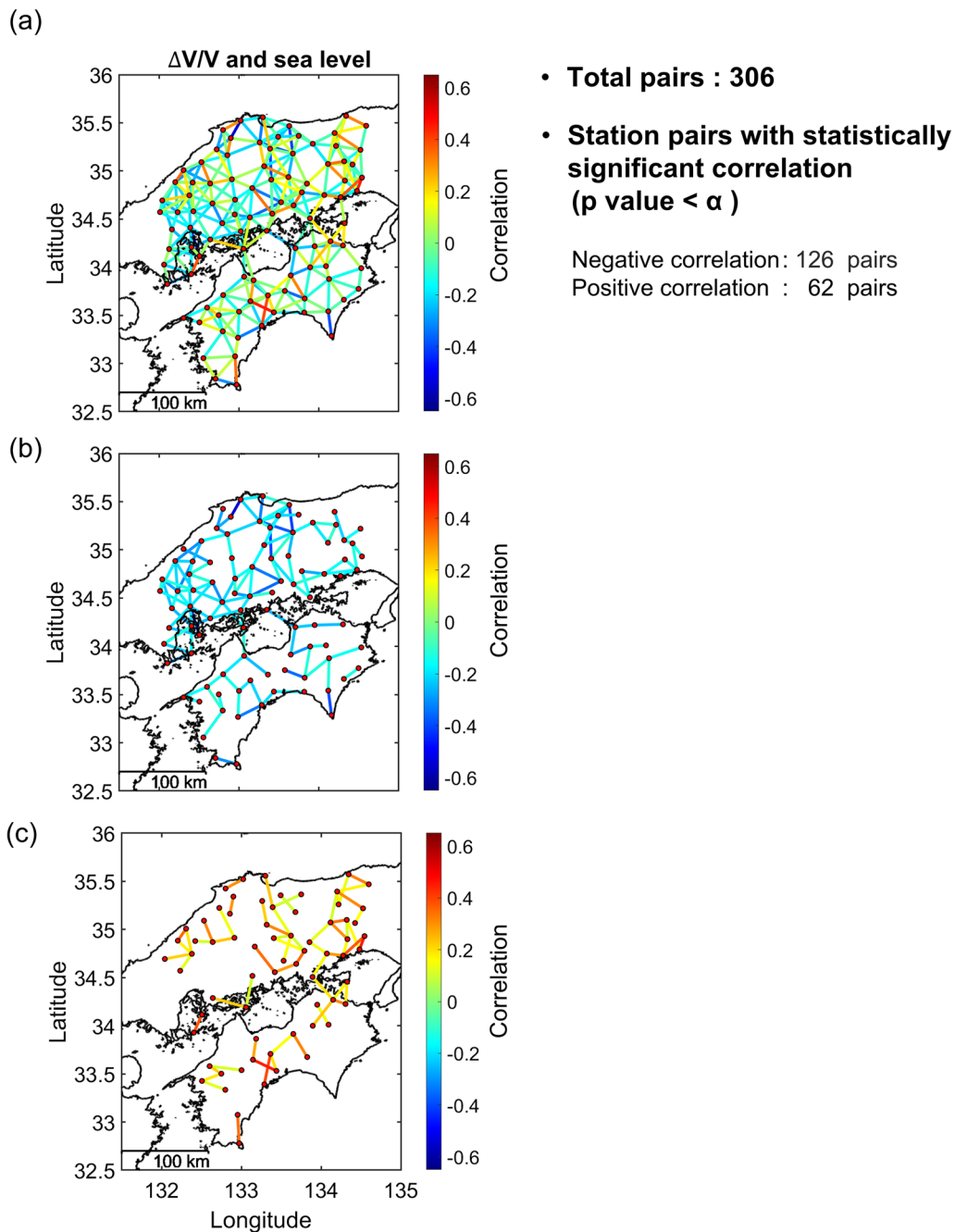


Fig. 9 Maps of the study region showing correlations between seismic velocity change and sea level for **a** all seismic station pairs, **b** station pairs with statistically significant negative correlations, and **c** station pairs with statistically significant positive correlations. Seismic velocity changes and sea level data are filtered within the 64- to 274-day period band

emphasized by the regional features of the average correlations, where the correlation between seismic velocity change and sea level change tends to be stronger near coastal regions (Fig. 8).

Comparison with non-oceanic perturbations

To validate if the selected period band could represent the sea level influence on seismic velocity changes, we compared our result with those for other environmental

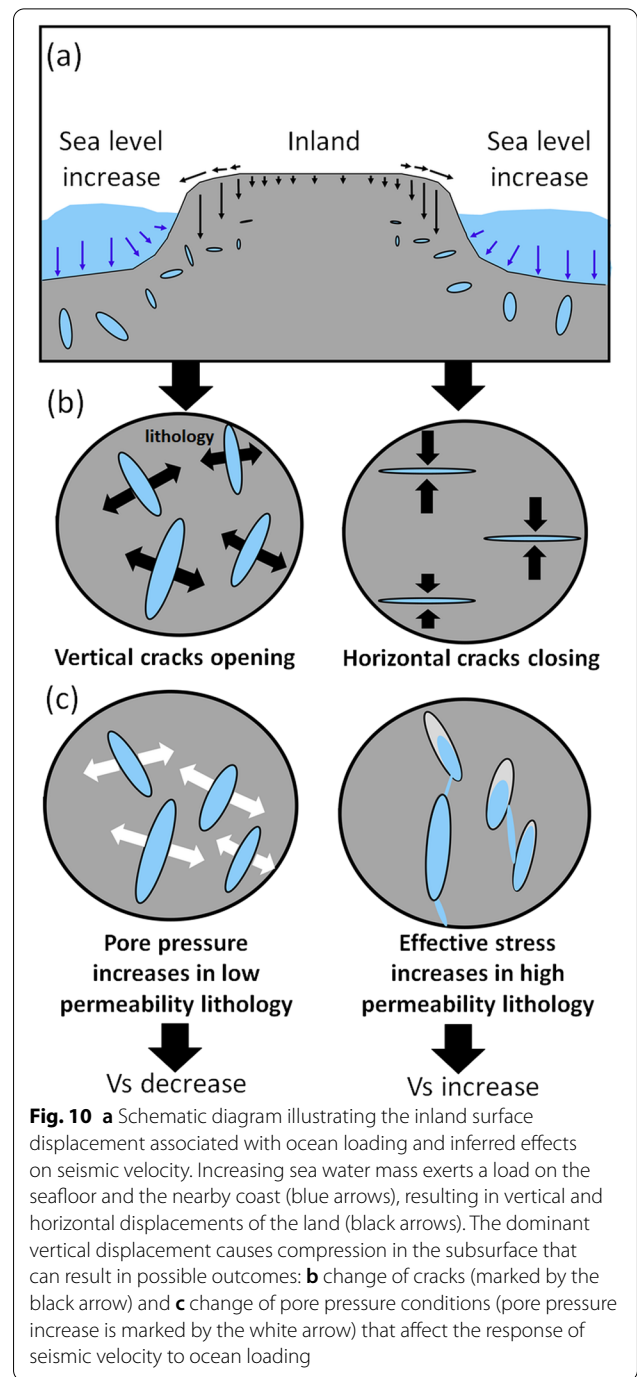
variables. Figure 7b shows a scatterplot of atmospheric pressure versus seismic velocity changes, using the same period band. This plot displays no appreciable trend nor statistically significance ($R=0.14$ with p -value=0.2), indicating that the trend in Fig. 7a is unlikely to reflect the perturbation from the atmospheric pressure.

We also considered whether rainfall could account for the negative trend like the one shown in Fig. 7a. Rainfall requires an infiltration process to influence seismic velocity change. For periods between 64 – 274 days, the precipitation cycle at most precipitation gauges tends to be similar to the sea level cycle, especially in northern Chugoku and central Shikoku (Additional file 1: Figure S5). This similarity makes it difficult to evaluate the possibility of an infiltration effect (Andajani et al. 2020). A comparison of total annual precipitation at each gauge and its proximity to the coast (Additional file 1: Figure S6) shows that some stations within 20 km of the coast have higher total annual precipitation than other stations and thus could be susceptible to rainfall perturbations. However, the absence of a clear trend between total precipitation and distance from the coast means that the decreasing trend in Fig. 7 is not associated with the amount of precipitation.

We also compared the magnitude of other perturbations that can influence seismic velocity changes near the coast. Changes in atmospheric pressure as large as $\sim 10^3$ Pa have been shown to cause temporal variations in seismic velocity at various depths (Silver et al. 2007; Niu et al. 2008). Assuming that the amplitudes of the Earth tide and ocean tide are similar, the amplitude of the 0.5-year period in the study region is ~ 1.7 cm (Japan Coast Guard 2021), corresponding to ~ 170 Pa. Our calculations for the 64- to 274-day period band show that changes in atmospheric pressure amount to ~ 800 Pa, while the change in the sea level is ~ 17 cm (the red line in the Additional file 1: Figure S2c and d) that equals ~ 1700 Pa. These comparisons show that the magnitude of the sea-level change is larger than the contribution from atmospheric pressure variations and earth tides. Therefore, the external forcing in the period band of 64 – 274 days is likely to be dominated by the perturbation from the ocean.

Interpretation of the mechanism

The selected period range from 64 – 274 days registers the influence of sea level at the coast, which may be due to several factors such as river runoff, seasonal changes in mean sea level, and tides (Fig. 2 in Woodworth et al. 2019). Variations in sea level are known to deform the lithosphere and cause surface displacements (e.g., Neumeier et al. 2005; van Dam et al. 1997). Ocean loading bends the land, pushing the crust downward and



subjecting the upper crust to dilation. Given that seismic velocity estimated from coda waves is sensitive to external loads (e.g., Grêt et al. 2006; Wang et al. 2008), seismic velocity changes could be ascribed to inland stress changes due to sea level variation.

Adding or removing masses of water can deform the Earth’s crust and cause surface displacements. For

example, removing water equivalent to a layer 1 m thick in an area of 20 km radius can cause vertical and horizontal displacements for several millimeters at sites located at tens of kilometers from the source (Fig. 1 in Wahr et al. 2013). We observed negative correlations as strong as -0.4 between sea level and seismic velocity changes around 25 km from the coast (Appendix Fig. S3) and positive correlations as strong as ~ 0.3 within 15.6 km from the coast (Appendix Fig. S4). Non-tidal ocean loading is known to influence the GPS sites within 50 km of the ocean (e.g., van Dam et al. 1997). All of the seismic stations in our study region, being less than 50 km from the coast, were considered subject to effects of ocean loading.

Vertical and horizontal deformation due to ocean loading reflect changes in vertical stress and inland bending. Geodetic studies based on GPS signals show that vertical displacements from movements of a concentrated mass (e.g., mass discharge to the ocean) tend to be larger than horizontal displacements (van Dam et al. 1997; Wahr et al. 2013). Considering this, we assumed that vertical stress changes produce the dominant effect on the land by the mechanism depicted in Fig. 10a: as sea level rises, the seawater mass exerts a load on the seafloor and the adjacent land area (the blue arrows) such that the upper crust shifts downward and toward the ocean (the black arrows). The combined effect of these movements causes vertical compression in the subsurface.

Possible factors that cause the variation in the seismic velocity change

Many factors can generate positive and negative correlations between seismic velocity change and sea level variability related to ocean loading (Fig. 9). Here, we consider several possible factors that may cause such variations, for example, the in situ stress state, the orientation of cracks, and hydraulic conductivity.

The first possibility is that seismic velocity change reflects the stress state (i.e., effective stress and pore pressure) induced by the sea level variability. Ocean loading is known to perturb stress both offshore and onshore. Considering that the present in situ stress is influenced by geological features such as faults and folds, the stress conditions are likely to vary in different areas. Thus, the oceanic perturbation can cause onshore stress to increase or decrease, which can cause either a positive or negative correlation between seismic velocity change and sea level.

Next, the variation in the seismic velocity can also be influenced by the presence and the orientation of cracks. Depending on the crack orientation, cracks can introduce seismic anisotropy. Cracks can be deformed (close or open) because of the stress induced by the ocean loading.

Here, we assume that the coda signal used in estimating seismic velocity changes is dominated by the energy of surface (Rayleigh) waves (e.g., Obermann et al. 2015; Wu et al. 2016). The surface wave velocity is associated with shear wave velocity (Xia et al. 1999), which in turn is sensitive to the opening and closing of microcracks. The seismic velocity changes in our study region mostly reflect the temporal variation of S-wave velocities within the 1.5–2 km depth range (Andajani et al. 2020). It is possible to interpret seismic velocity changes in terms of the opening or closure of microcracks due to stress changes imposed by ocean loading. Suppose the vertical stress change is dominant on the land, the cracks will close if the dominant cracks are horizontal, whereas these cracks will open if they are closer to the vertical (Fig. 10b). Thus, these crack orientations may explain both positive and negative correlations between seismic velocity and sea level.

Finally, we consider the contribution of fluid hydraulic conductivity with the change of vertical stress. Depending on lithologic conditions, the correlation between seismic velocity change and sea level change may be positive or negative. For example, in relatively impermeable rocks, the increase of vertical compression can increase pore pressure to the point of generating cracks (white arrows in Fig. 10c). This reduces the seismic velocity, resulting in a negative correlation between seismic velocity change and sea level. The vertical stress change can also increase the rock's effective stress if the pore pressure is negative or fluid flows out in highly permeable rocks. This causes the seismic velocity to increase. This results in a positive correlation between seismic velocity change and sea level change.

We concluded that temporal changes in seismic velocity could be dominated by external perturbations, including sea level variability. Our analysis suggests that the crust closer to the coast can be susceptible to the ocean loading. The absolute correlation between seismic velocity change and sea level change decreased with increasing seismic station distance from the coast. Ocean loading marked by sea level increase caused the land local stress to change. In situ stress condition, fracture orientation, and fluid role likely contribute to the seismic velocity change. Note that this study is still an exploratory work as our interpretation is based on a simple model that ignores many tidal and non-tidal factors and steric effects that affect sea level. To better evaluate the stress change at coastal areas related to the sea level increase, further analysis should be carried out by comparing the seismic velocity monitoring with a quantitative model of the ocean mass redistribution around the Chugoku Shikoku regions.

Conclusion

In this study, we analyzed temporal changes in seismic velocity from ambient noise to evaluate the imprint of temporal changes in crustal conditions related to environmental loading on observed changes in shear velocity. Our results support the hypothesis that seismic velocity changes in coastal regions are affected by variations in sea level. By taking into account the station's proximity to the coast, we were able to emphasize the imprint of sea level in seismic velocity changes. A statistical analysis revealed that the absolute correlation between ocean perturbation and seismic velocity tends to decrease with increasing distance from the coast. We show that consideration of station's distance from the coast helps to distinguish the influence of sea level on seismic velocity monitoring. Our primary conclusions are:

- (1) Variations in sea level may influence seismic velocity changes through the shallow crustal deformation induced by ocean loading. This is consistent with the decreasing strength of the absolute correlation between sea level and seismic velocity change with increasing distance from the coast.
- (2) The imprint of sea-level variability on seismic velocity changes persists at least up to dozens of kilometers inland from the coast.
- (3) The increase of sea level deforms the ocean bottom and causes the land to experience vertical compression in the subsurface. The resulting inland local stress changes influence seismic velocity changes.
- (4) Depending on the inland crack's orientation, the correlation between seismic velocity change and sea level can be either negative or positive. With the dominant vertical stress change, if the dominant cracks are perpendicular to the vertical stress, the cracks will open as sea level increases (negative correlation with sea level). On the other hand, if the dominant cracks are parallel to the vertical stress, the cracks will close (positive correlation with sea level).
- (5) Lithology condition contributes to the correlation between seismic velocity change and sea level. A positive correlation may reflect cracks closure related to increased effective stress caused by negative pore pressure or fluid loss in highly permeable rock as the subsurface is vertically compressed. Meanwhile, a negative correlation implies cracks generation because of increased pore pressure in low-permeability rocks.

Supplementary Information

The online version contains supplementary material available at <https://doi.org/10.1186/s40623-022-01657-8>.

Additional file 1: Figure S1. The map of stretching correlation coefficient for each seismic station pair. **Figure S2.** The time series of (a) sea level and atmospheric pressure (b) from all measurement stations. Panel c and d shows the unfiltered and filtered time series of the averaged sea level and atmospheric pressure, respectively. **Figure S3.** Examples of time series of seismic velocity change (blue) and sea level (black) for station pairs (a–d) with negative correlations. **Figure S4.** Examples of time series of seismic velocity change (blue) and sea level (black) for station pairs (a–d) with positive correlations. **Figure S5.** The time series of (a) the averaged sea level along the coast and (b) its comparison with the time series of the selected precipitation gauge. Panel c shows the correlation between the filtered sea level and the precipitation in 64–274 period band. **Figure S6.** The scatterplot between total annual precipitation and the measurement gauge's distance from the coast. Panel (a–c) shows the total annual precipitation for year 2015, 2016, 2017, respectively.

Additional file 2: Table S1. Result for all possible period bands estimated from Step 1.

Acknowledgements

We used Hi-net seismic data from the National Research Institute for Earth Science and Disaster Resilience (NIED). We obtained rainfall, sea level, and atmospheric pressure data from the Japan Meteorological Agency (JMA). We appreciate Fernando Lawrens Hutapea (Kyushu Univ.) for his technical support in computing seismic velocity change. This study was also supported by Japan Society for the Promotion of Science grants (no. JP20H01997). We are grateful for the support provided by the Advanced Graduate Program in Global Strategy for Green Asia of Kyushu University, and International Institute for Carbon-Neutral Energy Research (I2CNER) funded by the World Premier International Research Center Initiative of the Ministry of Education, Culture, Sports, Science and Technology, Japan (MEXT).

Author contributions

RDA proposed this study and drafted the initial manuscript. TT, RS, and TI suggested the method for the interpretation, and revised the manuscript. All authors read and approved the final manuscript.

Funding

This work was supported by Japan Society for the Promotion of Science grants (no. JP20H01997 and JP21H05202).

Availability of data and materials

Seismic data required to evaluate the conclusions in the paper are available from NIED (http://www.hinet.bosai.go.jp/about_data/?LANG=en). The meteorological data were obtained from JMA (<https://www.jma.go.jp/jma/index.html>).

Declarations

Competing interests

The authors declare that they have no competing interests.

Author details

¹Department of Systems Innovation, The University of Tokyo, 731 Hongo Bunkyo-ku, Tokyo 113-8656, Japan. ²Department of Earth Resources Engineering, Kyushu University, 744 Motoooka, Nishi-ku, Fukuoka 819-0395, Japan. ³International Institute for Carbon-Neutral Energy Research (WPI-I2CNER),

Kyushu University, 744 Motoooka, Nishi-ku, Fukuoka 819-0395, Japan. ⁴Colorado School of Mines, Golden, CO 80401-1887, USA.

Received: 6 November 2021 Accepted: 5 June 2022
Published online: 20 June 2022

References

- Akoglu H (2018) User's guide to correlation coefficients. *Turkish Journal of Emergency Medicine* 18(3):91–93. <https://doi.org/10.1016/j.tjem.2018.08.001>
- Albino F, Pinel V, Sigmundsson F (2010) Influence of surface load variations on eruption likelihood: application to two Icelandic subglacial volcanoes. *Grimsvötn and Katla Geophysics J Int* 181(3):1510–1524. <https://doi.org/10.1111/j.1365-246X.2010.04603.x>
- Andajani RD, Tsuji T, Snieder R, Ikeda T (2020) Spatial and temporal influence of rainfall on crustal pore pressure based on seismic velocity monitoring. *Earth, Planets Sp* 72(1):117. <https://doi.org/10.1186/s40623-020-01311-1>
- Donaldson C, Winder T, Caudron C, White RS (2019) Crustal seismic velocity responds to a magmatic intrusion and seasonal loading in Iceland's Northern Volcanic Zone. *Sci Adv* 5(11):eaax6642. <https://doi.org/10.1126/sciadv.aax6642>
- Geological Survey of Japan, AIST (ed.) (2015) Seamless digital geological map of Japan 1:200,000. May 29, 2015 version. Geological Survey of Japan, National Institute of Advanced Industrial Science and Technology. <https://gbank.gsj.jp/geonavi/>. Accessed 10 Feb 2021.
- Gladkikh V, Tenzer R, Denys P (2011) Crustal Deformation due to Atmospheric Pressure Loading in New Zealand. *J Geod Sci* 1(3):271–279. <https://doi.org/10.2478/v10156-011-0005-z>
- Grêt A, Snieder R, Scales J (2006) Time-lapse monitoring of rock properties with coda wave interferometry. *J Geophys Res Solid Earth* 111(B3). <https://doi.org/10.1029/2004JB003354>
- Hadziioannou C, Larose E, Coutant O, Roux P, Campillo M (2009) Stability of monitoring weak changes in multiply scattering media with ambient noise correlation: Laboratory experiments. *J Acoust Soc Am* 125(6):3688–3695. <https://doi.org/10.1121/1.3125345>
- Haigh ID (2017) Tides and Water Levels. In: Carlton J, Jukes P, Choo YS (eds) *Encyclopedia of Maritime and Offshore Engineering*. John Wiley & Sons, Ltd, Chichester, UK, pp 1–13. <https://doi.org/10.1002/9781118476406.emoe122>
- Hatanaka Y, Sengoku A, Sato T, et al (2001) Detection of Tidal Loading Signals from GPS Permanent Array of GSI Japan. *J Geod Soc Japan* 47(1):187–192. <https://doi.org/10.11366/sokuchii1954.47.187>
- Hillers G, Ben-Zion Y, Campillo M, Zigone D (2015) Seasonal variations of seismic velocities in the San Jacinto fault area observed with ambient seismic noise. *Geophys J Int* 202(2):920–932. <https://doi.org/10.1093/gji/ggv151>
- Hobiger M, Wegler U, Shiomi K, Nakahara H (2012) Coseismic and postseismic elastic wave velocity variations caused by the 2008 Iwate-Miyagi Nairiku earthquake, Japan. *J Geophys Res Solid Earth* 117(B9). <https://doi.org/10.1029/2012JB009402>
- Hunt L, Hadley S, Reynolds S, et al (2014) Precise 3D seismic steering and production rates in the Wilrich tight gas sands of West Central Alberta. *Interpretation* 2(2):SC1–SC18. <https://doi.org/10.1190/INT-2013-0086.1>
- Hutapea FL, Tsuji T, Ikeda T (2020) Real-time crustal monitoring system of Japanese Islands based on spatio-temporal seismic velocity variation. *Earth, Planets Sp* 72(1):19. <https://doi.org/10.1186/s40623-020-1147-y>
- Ikeda H & Takagi R (2019). Coseismic changes in subsurface structure associated with the 2018 Hokkaido eastern Iburi earthquake detected using autocorrelation analysis of ambient seismic noise. *Earth, Planets and Space*, 71(1). <https://doi.org/10.1186/s40623-019-1051-5>
- Ikeda T, Tsuji T (2018) Temporal change in seismic velocity associated with an offshore MW 5.9 Off-Mie earthquake in the Nankai subduction zone from ambient noise cross-correlation. *Prog Earth Planet Sci* 5(1):62. <https://doi.org/10.1186/s40645-018-0211-8>
- Japan Coast Guard (JCG) (2021) Hydrographic and Oceanographic Department. https://www1.kaiho.mlit.go.jp/TIDE/gauge/index_eng.php. Accessed 10 Feb 2021.
- Kalkomey CT (1997) Potential risks when using seismic attributes as predictors of reservoir properties. *Lead Edge* 16(3):247–251. <https://doi.org/10.1190/1.1437610>
- Khandelwal M (2013) Correlating P-wave Velocity with the physico-mechanical properties of different rocks. *Pure Appl Geophys* 170(4):507–514. <https://doi.org/10.1007/s00024-012-0556-7>
- Kim JH, Choi I (2019) Choosing the Level of Significance: A Decision-theoretic Approach. *Abacus* 57(1):27–71. <https://doi.org/10.1111/abac.12172>
- Matthews AJ, Barclay J, Johnstone JE (2009) The fast response of volcano-seismic activity to intense precipitation: triggering of primary volcanic activity by rainfall at Soufrière Hills Volcano, Montserrat *J Volcanol Geotherm Res* 184(3):405–415. <https://doi.org/10.1016/j.jvolgeores.2009.05.010>
- McBeck J, Ben-Zion Y, Renard F (2020) The mixology of precursor strain partitioning approaching brittle failure in rocks. *Geophys J Int* 221(3):1856–1872. <https://doi.org/10.1093/gji/ggaa121>
- Meier U, Shapiro NM, Brenguier F (2010) Detecting seasonal variations in seismic velocities within Los Angeles basin from correlations of ambient seismic noise. *Geophys J Int* 181:985–996. <https://doi.org/10.1111/j.1365-246X.2010.04550.x>
- Minato S, Tsuji T, Ohmi S, Matsuoka T (2012) Monitoring seismic velocity change caused by the 2011 Tohoku-oki earthquake using ambient noise records. *Geophys Res Lett* 39(9). <https://doi.org/10.1029/2012GL051405>
- Mordret A, Mikesell TD, Harig C et al (2016) Monitoring southwest Greenland's ice sheet melt with ambient seismic noise. *Sci Adv* 2(5):e1501538. <https://doi.org/10.1126/sciadv.1501538>
- Nakata N, Snieder R (2012) Estimating near-surface shear wave velocities in Japan by applying seismic interferometry to KIK-net data. *J Geophys Res Solid Earth* 117(B1). <https://doi.org/10.1029/2011JB008595>
- Neuberg J (2000) External modulation of volcanic activity. *Geophys J Int* 142(1):232–240. <https://doi.org/10.1046/j.1365-246X.2000.00161.x>
- Neumeyer J, del Pino J, Dierks O et al (2005) Improvement of ocean loading correction on gravity data with additional tide gauge measurements. *J Geodyn* 40(1):104–111. <https://doi.org/10.1016/j.jjog.2005.07.012>
- Nimiya H, Ikeda T, Tsuji T (2017) Spatial and temporal seismic velocity changes on Kyushu Island during the 2016 Kumamoto earthquake. *Sci Adv* 3(11):e1700813. <https://doi.org/10.1126/sciadv.1700813>
- Niu F, Silver PG, Daley TM et al (2008) Preseismic velocity changes observed from active source monitoring at the Parkfield SAFOD drill site. *Nature* 454(7201):204–208. <https://doi.org/10.1038/nature07111>
- Obara K, Kasahara K, Hori S, Okada Y (2005) A densely distributed high-sensitivity seismograph network in Japan: Hi-net by National Research Institute for Earth Science and Disaster Prevention. *Rev Sci Instrum* 76(2):21301. <https://doi.org/10.1063/1.1854197>
- Obermann A, Kraft T, Larose E, Wiemer S (2015) Potential of ambient seismic noise techniques to monitor the St. Gallen geothermal site (Switzerland). *J Geophys Res Solid Earth* 120(6):4301–4316. <https://doi.org/10.1002/2014JB011817>
- Pacheco C, Snieder R (2005) Time-lapse travel time change of multiply scattered acoustic waves. *J Acoust Soc Am* 118(3):1300–1310. <https://doi.org/10.1121/1.2000827>
- Pacheco C, Snieder R (2006) Time-lapse traveltime change of singly scattered acoustic waves. *Geophys J Int* 165(2):485–500. <https://doi.org/10.1111/j.1365-246X.2006.02856.x>
- Richter T, Sens-Schönfelder C, Kind R, Asch G (2014) Comprehensive observation and modeling of earthquake and temperature-related seismic velocity changes in northern Chile with passive image interferometry. *J Geophys Res Solid Earth* 119(6):4747–4765. <https://doi.org/10.1002/2013JB010695>
- Rivet D, Brenguier F, Clarke D et al (2014) Long-term dynamics of Piton de la Fournaise volcano from 13 years of seismic velocity change measurements and GPS observations. *J Geophys Res Solid Earth* 119(10):7654–7666. <https://doi.org/10.1002/2014JB011307>
- Sato T, Fukuda Y, Aoyama Y et al (2001) On the observed annual gravity variation and the effect of sea surface height variations. *Phys Earth Planet Inter* 123(1):45–63. [https://doi.org/10.1016/S0031-9201\(00\)00216-8](https://doi.org/10.1016/S0031-9201(00)00216-8)
- Schober P, Boer C, Schwarte LA (2018) Correlation coefficients. Appropriate use and interpretation. *Anesth Analg* 126(5):1763–1768. <https://doi.org/10.1213/ane.0000000000002864>
- Sens-Schönfelder C, Wegler U (2006) Passive image interferometry and seasonal variations of seismic velocities at Merapi Volcano, Indonesia. *Geophys Res Lett* 33(21). <https://doi.org/10.1029/2006GL027797>
- Silver PG, Daley TM, Niu F, Majer EL (2007) Active source monitoring of cross-well seismic travel time for stress-induced changes. *Bull Seismol Soc Am* 97(1B):281–293. <https://doi.org/10.1785/0120060120>

- Suemoto Y, Ikeda T, Tsuji T, Iio Y (2020) Identification of a nascent tectonic boundary in the San-in area, southwest Japan, using a 3D S-wave velocity structure obtained by ambient noise surface wave tomography. *Earth Planets Space* 72:15. <https://doi.org/10.1186/s40623-020-1139-y>
- Takano T, Nishimura T, Nakahara H (2017) Seismic velocity changes concentrated at the shallow structure as inferred from correlation analyses of ambient noise during volcano deformation at Izu-Oshima. *Japan J Geophys Res Solid Earth* 122(8):6721–6736. <https://doi.org/10.1002/2017JB014340>
- Thiese MS, Ronna B, Ott U (2016) P value interpretations and considerations. *J Thorac Dis* 8(9):E928–E931. <https://doi.org/10.21037/jtd.2016.08.16>
- van Dam TM, Blewitt G, Heflin MB (1994) Atmospheric pressure loading effects on global positioning system coordinate determinations. *J Geophys Res* 99(B12):23939–23950. <https://doi.org/10.1029/94jb02122>
- van Dam TM, Wahr J, Chao Y, Leuliette E (1997) Predictions of crustal deformation and of geoid and sea-level variability caused by oceanic and atmospheric loading. *Geophys J Int* 129(3):507–517. <https://doi.org/10.1111/j.1365-246X.1997.tb04490.x>
- Wahr J, Khan SA, Van Dam T et al (2013) The use of GPS horizontals for loading studies, with applications to northern California and southeast Greenland. *J Geophys Res Solid Earth* 118(4):1795–1806. <https://doi.org/10.1002/jgrb.50104>
- Wang Q-Y, Brenguier F, Campillo M et al (2017) Seasonal Crustal Seismic Velocity Changes Throughout Japan. *J Geophys Res Solid Earth* 122(10):7987–8002. <https://doi.org/10.1002/2017JB014307>
- Wang B, Zhu P, Chen Y, et al (2008) Continuous subsurface velocity measurement with coda wave interferometry. *J Geophys Res Solid Earth* 13(B12). <https://doi.org/10.1029/2007JB005023>
- Woodworth PL, Melet A, Marcos M et al (2019) Forcing Factors Affecting Sea Level Changes at the Coast. *Surv Geophys* 40(6):1351–1397. <https://doi.org/10.1007/s10712-019-09531-1>
- Wu C, Delorey A, Brenguier F et al (2016) Constraining depth range of S wave velocity decrease after large earthquakes near Parkfield. *California Geophys Res Lett* 43(12):6129–6136. <https://doi.org/10.1002/2016GL069145>
- Xia J, Miller RD, Park CB (1999) Estimation of near-surface shear-wave velocity by inversion of Rayleigh waves. *Geophysics* 64(3):691–700. <https://doi.org/10.1190/1.1444578>
- Yukutake Y, Ueno T, & Miyaoka K (2016). Determination of temporal changes in seismic velocity caused by volcanic activity in and around Hakone volcano, central Japan, using ambient seismic noise records. *Progress in Earth and Planetary Science*, 3(1). <https://doi.org/10.1186/s40645-016-0106-5>

Publisher's Note

Springer Nature remains neutral with regard to jurisdictional claims in published maps and institutional affiliations.

Submit your manuscript to a SpringerOpen[®] journal and benefit from:

- Convenient online submission
- Rigorous peer review
- Open access: articles freely available online
- High visibility within the field
- Retaining the copyright to your article

Submit your next manuscript at ► [springeropen.com](https://www.springeropen.com)
